Ion permeation dynamics in carbon nanotubes

Hongmei Liu and Sohail Murad[a)]
Department of Chemical Engineering, University of Illinois at Chicago, Chicago, Illinois 60607

Cynthia J. Jameson
Department of Chemistry, University of Illinois at Chicago, Chicago, Illinois 60607
and Department of Chemical Engineering, University of Illinois at Chicago, Chicago, Illinois 60607

(Received 31 May 2006; accepted 20 July 2006; published online 25 August 2006)

Molecular dynamics simulations are carried out to investigate the permeation of ions and water in a membrane consisting of single wall carbon nanotubes possessing no surface charges connecting two reservoirs. Our simulations reveal that there are changes in the first hydration shell of the ions upon confinement in tubes of 0.82 or 0.90 nm effective internal diameter. Although the first minimum in the $g(r)$ is barely changed in the nanotube compared to in the bulk solution, the hydration number of Na^+ ion is reduced by 1.0 (from 4.5 in bulk to 3.5 in the 0.90 nm tube) and the hydration number is reduced further in the 0.82 nm tube. The changes in the hydration shell of Cl^- ion are negligible, within statistical errors. The water molecules of the first hydration shell of both ions exchange less frequently inside the tube than in the bulk solution. We compare ion trajectories for ions in the same tube under identical reservoir conditions but with different numbers of ions in the tubes. This permits investigation of changes in structure and dynamics which arise from multiple ion occupancy in a carbon nanotube possessing no surface charges. We also investigated the effects of tube flexibility. Ions enter the tubes so as to form a train of ion pairs. We find that the radial distribution profiles of Na^+ ions broaden significantly systematically with increasing number of ion pairs in the tube. The radial distribution profiles of Cl^- ions change only slightly with increasing number of ions in the tube. Trajectories reveal that Na^+ ions do not pass each other in 0.90 nm tubes, while Cl^- ions pass each other, as do ions of opposite charge. An ion entering the tube causes the like-charged ions preceding it in the tube to be displaced along the tube axis and positive or negative ions will exit the tube only when one or two other ions of the same charge are present in the tube. Thus, the permeation mechanism involves multiple ions and Coulomb repulsion among the ions plays an essential role. © *2006 American Institute of Physics*. [DOI: 10.1063/1.2337289]

I. INTRODUCTION

Specialized transmembrane proteins form channels that facilitate the transport of ions and other molecules across membranes and thus play crucial roles in vital cellular functions. The understanding of these systems has increased in recent years because of advances in structural and biochemical studies.[1–4] However, key questions remain with regards to the exact factors that control the selectivity and gating of ion transport across membranes. To understand these factors, it would be very useful to quantify the energy contributions that allow some ions to permeate while blocking others. Availability of structural information is of course crucial, for example, the recent availability of x-ray structures for anionic channels[5,6] has spurred theoretical investigations.[7–10] Computational simulation studies using these structures as starting points help to address some issues and generate hypotheses and models for gating, selectivity, and mechanisms of permeation. Do the orientations of the water molecules control the ion transport? What about the electrostatic interactions between the ion and the channel? Is the electrostatics governed by specific residues in the mouth of the channel, in the center of the channel? What is the nature of the electrostatic barriers that governs ion penetration in transmembrane channels? To what extent do the dynamics of the protein play a role in gating, selectivity, and permeation? These are very complex systems so it is difficult to answer these questions.

There is a clear need for well-defined experimental test cases to guide the understanding of ion selectivity and the dynamics of the transport mechanism. Mutation studies[11] pave the way for detailed scrutiny of different hypotheses and models. However, mutation studies sometimes pose more questions rather than provide immediate answers. A single mutation is capable of changing the protein structure such as to widen the pore and permit water molecules to penetrate and stabilize the ion within the channel. Or the mutation may lead to rearrangement of dipoles and charges that will change the electrostatic barrier for ion transport. The mechanism by which a mutation can cause the channel to be nonfunctional can be due to either of these or arise from some other structural and dynamic changes. In contrast, loss of solvation energy upon transfer of the ion from the bulk solvent to the channel interior is sufficient to explain selective permeation of ions into simpler membranes such as zeolite membranes.[12,13] Pores can pose high barriers to the permeation of ions, even when the pore radius is considerably larger than the ionic radius. The barrier originates in the

[a)]Electronic mail: murad@uic.edu

high energetic cost for an ion to shed its first or its second hydration shell. Therefore, there is something to be gained from studies in simple model systems. In simple channel systems, it is possible to study the effect of small changes in pore diameter and charge distributions in the channel walls on ion transport. Molecular dynamics studies of the detailed ion behavior in the bulk solvent in contrast to ion behavior within the confinement of simple channels can shed some light on more general details of ion transport, unencumbered by the complexity that is inherent in the actual transmembrane protein channel systems. Therefore, in this paper, we consider ion permeation of nanochannels as a general phenomenon and have carried out molecular dynamics (MD) studies of ion transport in model channels in order to help answer some of the questions from a more fundamental perspective before addressing the complexity and specificity of the protein channel systems. Simplified pore models permit investigation of the primary characteristics of a conduction pathway: the shape, radius, length of the pore, and the chemical (hydrophobic or hydrophilic) nature of the pore wall surface and its surface roughness and flexibility.

Carbon nanotubes serve as good atomistic models for nanochannels because it is possible to investigate the effects of varying the channel diameter without changing the nature of the atomic corrugation and surface density. We consider ions in solution in the bulk and we follow by molecular dynamics the penetration of ions from the bulk solution into the channels. We believe that the results from this simple system will help enlighten the refinement of electrostatic models for the energetics of ions in transmembrane ion channels. Furthermore, the parameters and mechanisms of permeation of ions in simple nanochannels are of interest in their own right in relation to material science and engineering problems. Recent advances in the fabrication of confined fluidic systems such as nanoscale lab-on-a-chip devices and nanofabricated pores[14] raise fundamental questions about ion transport in nanochannels. For example, the effects of nanoscale confinement on the transport properties of ions and water need to be resolved for the characterization and design of nanochannel-based devices. In particular, in the design of nanofluidic systems that use electro-osmotic transport as a primary means of fluidic transport[15–17] a detailed understanding of electro-osmotic transport in a hydrophobic nanotube is necessary. Solvent slip along the hydrophobic walls of the carbon nanotube is controlled by fluid-wall interactions. Investigation of such slip flow behavior and other characteristics of flow in nanotubes can be vital for generating the high throughput rates required in nanofluidic devices employing carbon nanotubes.[18]

Earlier molecular dynamics studies of permeation of water molecules into single-walled nanotubes have focused on the structure of the "water wire" or water chains inside carbon nanotubes of various sizes ranging from (5,5) to (9,9).[19–24] Radial density profiles and dipole orientation distributions have also been examined closely.[25] Grand canonical Monte Carlo simulations have been used to suggest mechanisms of pore filling and pore emptying.[26] Studies of water in smooth-wall tubes include investigations of diffusion coefficients, reorientation times, and average number of hydrogen bonds for water in tube compared to in bulk.[27–29] Other studies involved water permeation into carbon nanotubes with surface charges and/or in the presence of external electric fields or in osmotic flow.[30–33] A MD study of ion transport in a smooth cylindrical pore between two salt solution reservoirs has been published by Hansen and co-workers[34,35] since we started this work. They considered smooth cylindrical pores of various radii and characterized the behavior of water in pores. They also studied the approach to equilibrium and ion transport starting from different anion and cation concentrations in the reservoirs connected by the cylindrical pore. Under the influence of the ionic charge imbalance, water and ions permeate the pore. Both equilibrium MD and nonequilibrium molecular dynamics (NEMD) simulations of an electrolyte solution in a smooth-wall cylindrical pore were reported by Tang *et al.*[36] Like the earlier study of Lynden-Bell and Rasaiah[37] and Nicholson and Quirke,[38] their cylindrical tube is infinitely long. The present work differs from what has already been done by Hansen and co-workers[34,35] in that we study ion permeation in systems which are in quasisteady state and employ an atomistic dynamic (flexible) nanotube for our model channel. Since we started this work, a MD simulation of a sodium ion restrained near the center along the axial direction of a carbon nanotube has been published by Peter and Hummer.[39]

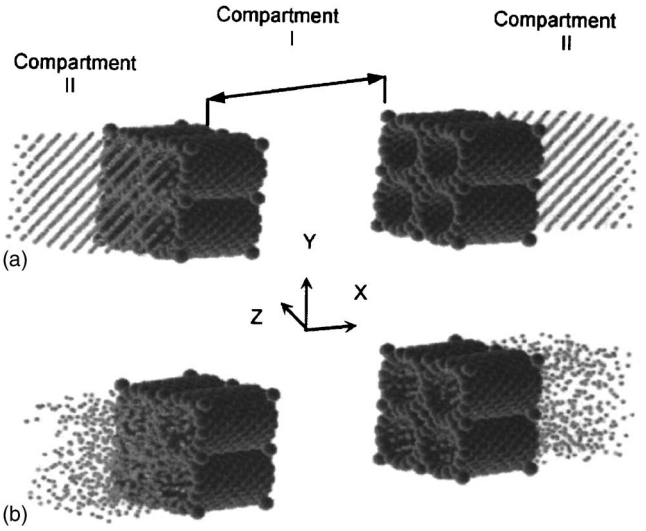

FIG. 1. The simulation box used in this work (a) at the outset and (b) at quasisteady state. The eight tubes which constitute the membranes are referred to as tubes 1–8 in all subsequent figures.

II. THE MODEL SYSTEM AND METHODS

Our simulation box is adopted from the model first introduced by one of us in 1993.[40] The simulation box consists of two compartments separated by two symmetric membranes. Periodic boundary conditions then lead to a system infinite in the y and z directions (parallel to the membranes). In the x direction, this leads to alternating compartment I and compartment II of width 6.84 nm. A schematic diagram is shown in Fig. 1.

Four carbon nanotubes of the zigzag type in a cubic arrangement constitute each membrane. In our simulations

TABLE I. Interaction parameters for potential models used. The ε and σ parameters of the cross interactions are calculated on the basis of the Lorentz-Berthelot combining rules.

Interacting sites	σ (10^{-10} m)	ε (kJ/mol)	q (e)
Water			
O	3.17	0.65	−0.82
H	0.00	0.00	0.41
Membrane			
C	3.40	1.50	0.00
Ions			
Cl	4.42	0.49	−1.00
Na	1.90	6.69	1.00

the membranes are formed by tethering the carbon sites by a simple harmonic potential $[\Phi_T=(1/2)k\delta^2]$. Here δ corresponds to the distance between the center of mass of the tethered carbon and the tethering site and k, the tethering force constant, is set equal to 900 reduced units (based on Na^+ parameters, see Table I) or 277 N m^{-1} for most of the simulations, leading to a fairly rigid membrane. Dummy atoms (with parameters identical to those of carbon atoms) were placed strategically at the entrances to intertube regions of the membrane to prevent water molecules and ions from entering these regions, since we are not interested in the behavior of water and ions on the outside surface of the nanotubes.

At the beginning of the study, compartment I is vacuum, the tubes are empty, and compartment II is filled with a solution of NaCl (2.26 mol/l). Two types of tubes were used in this work. One is a (16,0) type which has a diameter of 1.235 nm. We also used a (15,0) type which has a diameter of 1.1578 nm. The effective internal diameters of these tubes are 0.90 and 0.82 nm, respectively, using 0.34 nm as the diameter of the carbon atoms. In order to confine as many as 3 Cl^- ions in a tube, we had to choose a proper length for the tubes, which is 2.36 nm.

The density and temperature of the liquid water or salt solution can be fixed to correspond to the state condition of interest. In this study, the density of water was set to 0.28 reduced units in order to have higher driving forces and allow the system to be in a quasisteady state during our simulation. This establishes the volume of the compartments once the number of water molecules to be included in the compartment is fixed. At the beginning of each simulation, the contents of the compartments are electrically neutral, and the membrane is likewise electrically neutral. Furthermore, the only partial charges assigned are those to the water molecules, and the ions carry their usual charges of $+e$ and $-e$. The membrane atoms are uncharged for the present study. Surface charges have an important role in governing ionic conductance. In a subsequent paper, we carry out separate studies using partially charged tube atoms, with net overall neutral nanotubes or else net overall charged nanotubes balanced by excess ions in the solution compartments. In the present work, compartment II consisted of typically 810 water molecules and 54 Na^+ and 54 Cl^- ions.

The simple point charge (SPC) model was used for liquid water in pure water and also in the salt solutions. The SPC potential had been shown to give reasonable agreement with a range of experimental observations in liquid water.[41] Lennard-Jones potentials were used with a spherical cutoff of 0.95 nm. The site-site interaction potential used is of the form

$$u_{ij}=4\varepsilon_{ij}[(r/\sigma)^{-12}-[(r/\sigma)^{-6}]+q_iq_j/r, \quad (1)$$

where ε and σ are Lennard-Jones parameters and r is the distance between the sites. The Coulombic interaction terms were included in the potential for charged sites only. Table I lists the model parameters for ions and water molecules. The Lennard-Jones energy (ε) and diameter (σ) parameters of the cross interactions are calculated on the basis of the Lorentz-Berthelot combining rules.

The molecules were given a Gaussian distribution corresponding to the desired temperature of 298 K. The temperature was subsequently held constant at 298 K using a Gaussian thermostat. The time evolution of this initial system setup was then followed using a fifth order predictor-corrector scheme for the translational motion, a fourth order predictor scheme,[42] and the quaternion formulation of the equations of rotational motion about the center of mass of the water molecules.[43] The simulation system was allowed to equilibrate for 10 000 time steps, followed by production runs for 300 000 time steps. We have a long run of 300 000 time steps with time unit $0.527\,72\times10^{-15}$ s, so our total simulation time is 0.158 ns. Coordinates (snapshots) are saved every 3000 time steps for analysis (trajectories of ions, particle distributions, density profiles, hydration shells, and radial distribution functions).

We incorporate the effects of flexibility of the channel on ion and water permeation by adjusting the tethering force constant. We do not attempt to reproduce vibrational modes of actual carbon nanotubes; instead we study the qualitative effects of lowering the tethering force constant by one order of magnitude to include a larger dynamic component in the membrane itself, i.e., to simulate a more flexible tube.

III. RESULTS

A. Distributions

1. Occupancy

Previous workers have monitored water occupancy (number of water molecules in the pore) as a function of run time to demonstrate intermittent filling in tubes which have a critical diameter of the order of 0.55 nm.[35,44–47] Our tubes have sufficiently large diameters to initiate filling and stay filled. When the system approaches a steady state, the number of water molecules held in each nanotube stays at a constant level of about 53.

2. Changes in the hydration shell due to confinement

The structure of Na^+ and Cl^- solutions has been previously investigated in simulation studies at various levels of sophistication,[48–53] including *ab initio* molecular dynamics,[54–56] and there is general agreement with respect to basic features at ambient conditions. However, the effects of confinement on these features have not yet been explored. In this

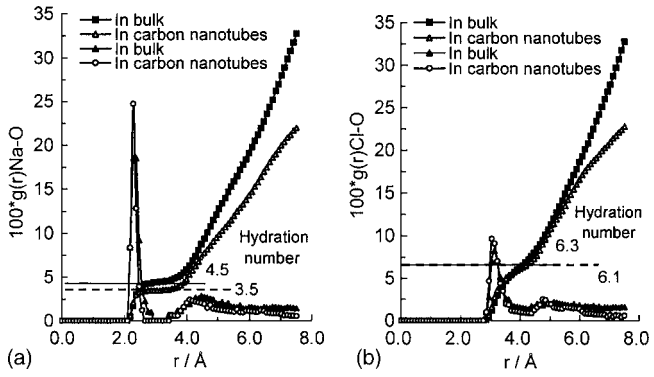

FIG. 2. (a) The Na–O radial distribution function inside the nanotube is compared with that in the bulk solution. The hydration numbers are taken at the position of the first minimum of $g(r)$, which are given in the figure. (b) The Cl–O radial distribution function inside the nanotube is compared with that in the bulk solution. The hydration number, taken at the position of the first minimum of $g(r)$, given in the figure, is indistinguishable from that in the bulk solution.

section we compare the distribution functions $g(r)$, the hydration shell structure, and the hydration number for the cation and the anion in the nanotube compared to these quantities in the bulk. The size of the first hydration shell is defined by the first minimum in the ion-oxygen radial distribution function, and this also defines the hydration number: the number of water oxygens located at a distance inside this first minimum.

In the Figs. 2(a), 2(b), 3(a), and 3(b), we examine the $g(r_{\mathrm{NaO}})$ and the $g(r_{\mathrm{ClO}})$ for ions inside the tube compared to the ions in the bulk. We find that the size of the first hydration shell of Na^+ ion is very nearly the same inside the tube as in the bulk, namely, 0.3040 nm in the carbon nanotube and 0.3135 nm in the bulk. For Cl^- ion, the size of the first hydration shell is very nearly the same inside the tube as in the bulk, about 0.3990 nm. From this figure we also obtain the hydration numbers. Although the boundaries of the first hydration shell of Na^+ in the carbon nanotube are the same as that in the bulk, the hydration number is smaller inside the tube than in the bulk, namely, 3.5 inside the tube compared to 4.5 in the bulk. The hydration number of the anion is difficult to ascertain precisely (the number is close to 6) because the integrated $g(r)$ does not have a plateau at the first minimum. As expected, the integrated $g(r)$ shows that there

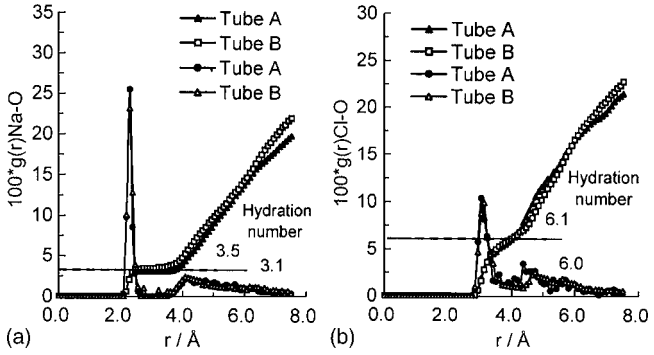

FIG. 3. The radial distribution functions inside two nanotubes of different diameters for (a) Na–O and (b) Cl–O. Effective diameter of tube A is 0.82 nm and of tube B is 0.90 nm.

are fewer water molecules beyond the first hydration shell in the nanotube in comparison to the bulk. [See Figs. 2(a) and 2(b).]

Our results in the bulk solution are very similar to the simulations of 1*m* NaCl solution in SPC water at 300 K by Driesner *et al.*;[48] for Na^+ ion the size of their first hydration shell is 0.31 nm and hydration number is 4.8; and for Cl^- ion, these are 0.40 nm and 8.3, respectively. Values obtained in various previous simulations in bulk solutions are in the ranges of 0.310–0.325 nm and 4.6–6.0 for Na^+ ion and 0.324–0.40 nm and 5.6–7.5 for Cl^- ion, and the position of the first maximum in $g(r)$ is in the ranges of 2.35–2.45 nm for Na^+ and 3.20–3.22 nm for Cl^- ion.[49–55]

We also examine the effect of the diameter of the tube on the size of the first hydration shell and the hydration number in Figs. 3(a) and 3(b). Comparing the results in tubes with diameters of 0.82 and 0.90 nm, we find that the diameter of the tube does not affect the size of the first hydration shell, but the smaller diameter tube has a smaller hydration number (3.1) for Na^+ ion. Again, as expected, the integrated $g(r)$ in Figs. 3(a) and 3(b) shows not only that there are fewer water molecules in the first hydration shell but also that there are fewer molecules in the second hydration shell of the Na^+ ion. On the other hand, for the Cl^- ion, which does not have a well-defined second minimum in its $g(r)$ even in the bulk solution, going to the somewhat smaller tube appears to stretch out the hydration shell so that the same number of waters is found within the region 0.5 nm from the center line of the tube in both the 0.82 and the 0.90 nm tubes. Although changes in the ion hydration structure can and do occur upon entering confined spaces, the energetic penalty for Na^+ ion to reduce the number of waters in its first hydration shell below a critical number prevents Na^+ ions from entering tubes of much smaller diameter.

3. Distribution of ions and water inside the tube: Radial profiles

Distribution profiles within a cross section of the channel, averaged over the length of the channel and time, are generated with a radial spacing of 0.1037 nm. These radial distribution profiles reveal the shell structure of the channel contents. We do not show the comparison of the radial distribution profiles of pure water as a function of tube diameter; this has been the subject of many other reports.[25,44,57,58] The radial distribution profiles of water and ions in infinitely long structureless cylindrical tubes of larger diameter have been reported by Nicholson and Quirke (in a 0.5*M* NaCl solution in tube diameters ranging from 1.3 to 3.94 nm)[38] and by Tang *et al.* (in a 0.5*M* KCl solution in tube diameters ranging from 0.95 to 3.16 nm).[36] Here we investigate the distribution of the ions within the tube and discover if this distribution is affected by the presence of other ions.

First we discuss the results which are general to all eight tubes and independent of the number of ions in the tube. A tube of this size (0.90 nm effective diameter) can support not only a central water column but also a cylindrical shell of water. Most water molecules reside in the cylindrical shell near the channel wall. We illustrate these general observations in Fig. 4 for the tube containing 2 Na^+ and 1 Cl^- ions.

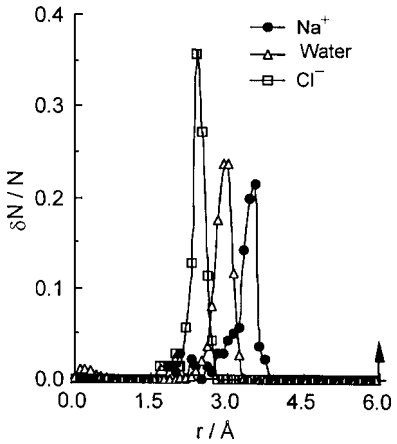

FIG. 4. Normalized radial particle distribution profiles ($\delta N/N$) for H_2O, Na^+ and Cl^- ions in the 0.90 nm tube as a function of radial distance from the axis of the tube. The numbers have been normalized to the number of particles in the tube, $2Na^+$, $1Cl^-$, and $54H_2O$. The wall of the tube is indicated by the arrow.

This is the radial distribution profile ($\delta N/N$ versus the radial distance from the center line) of O atoms of water and of Na^+ and Cl^- ions inside the tube, averaged over the sequence of the last 70 snapshots in a particular MD run in which the number of ions remains constant in the tube. The number of water molecules is much larger than the number of ions, so we normalized the particle densities by the average number present in the nanotube to produce Fig. 4. The maximum in the radial particle distribution profile for Na^+ is close to the outer water cylindrical shell. The radial profile for Cl^- ions in the nanotube has a maximum between the waters in the cylindrical shell and the waters along the center line. This is essential for Cl^- ion which usually has a hydration number larger than 6 inside the tube, in which the water molecules are loosely held. On the other hand, Na^+ ion usually has a tighter hydration shell with a hydration number between 4 and 5, and in this tube, Na^+ ion can satisfy this by being close to the cylindrical shell of water. Thus, the maximum of the Na^+ ion in the radial profile is close to the maximum for water. Tubes with diameters large enough to support both the central and cylindrical water shells permit Cl^- ions as well as Na^+ ions to permeate.

4. Distribution of ions and water inside the tube: Effect of the presence of other ions

Here we examine the effect of the presence of other ions on the radial distribution profile of an ion in the tube. We have considered the radial distribution profiles for each tube, comparing H_2O, Cl^-, and Na^+ ion distributions with one another. We find that the radial distribution profiles for water in the eight tubes are nearly identical in some respects for any number of ions present. In Fig. 4 we presented a typical radial distribution profile, $\delta N/N$ versus the distance from the centerline of the tube. The radial profiles for the ions are all slightly different, but we do not see any obvious systematic trends in the radial profiles of the Cl^- ion, for example, with the number of ions present.

Now to demonstrate the effect of the presence of other ions on the radial distribution profiles, we compare directly

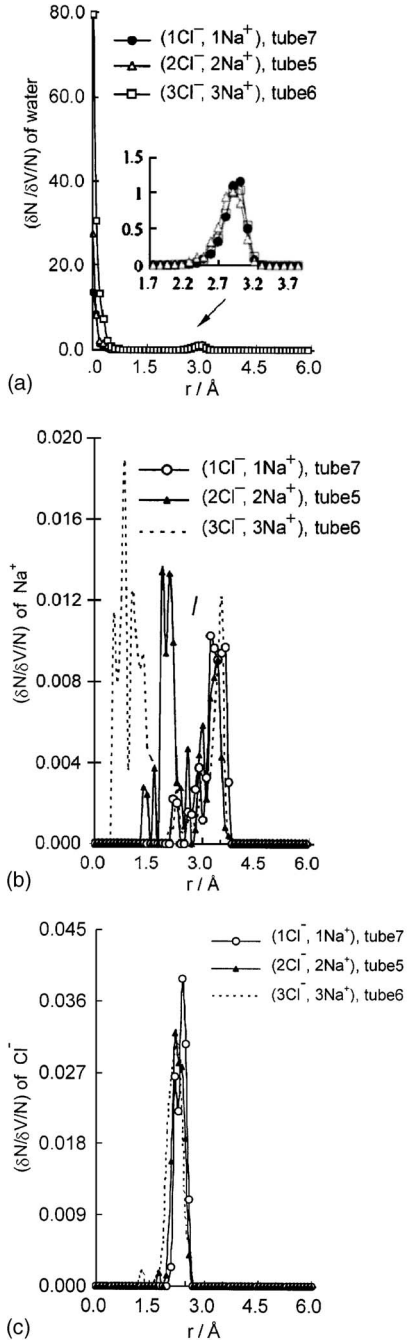

FIG. 5. Normalized radial particle density profiles (a) $(\delta N/\delta V)/N_{H_2O}$ comparison for H_2O in tube with $1Na^+$, $1Cl^-$ vs $2Na^+$, $2Cl^-$ vs $3Na^+$, $3Cl^-$. (b) $(\delta N/\delta V)/N_{Na^+}$ comparison for Na^+ ion in tube with $1Na^+$, $1Cl^-$, vs $2Na^+$ $2Cl^-$ vs $3Na^+$, $3Cl^-$. (c) $(\delta N/\delta V)/N_{Cl^-}$ comparison for Cl^- ion in tube with $1Na^+$, $1Cl^-$ vs $2Na^+$, $2Cl^-$ vs $3Na^+$, $3Cl^-$.

the results for one, two, or three ions of each kind in the same tube. We present the radial density profiles normalized to the number of molecules or ions, $(\delta N/\delta V)/N$ for H_2O in Fig. 5(a), for Cl^- ion in Fig. 5(c), and for Na^+ ion in Fig. 5(b).

The radial density profile of water has a shoulder towards the inside, and this shoulder is slightly different for different numbers of ion pairs. However, neither the width nor the maximum is systematically related to the number of ions present in the tube. On the other hand, the width of the radial profile of Na^+ ions is systematically related to the

number of ion pairs present in the tube. The width of the radial profile of Na^+ ion increases dramatically with the number of ion pairs present in the tube. The radial density profile of Cl^- ion is also systematically related to the number of ion pairs. The width is greater for 3 than for 2, which in turn is greater than for one ion pair, and the maximum shifts toward the center line with increasing number of ion pairs. The differences are consistent with, but not as dramatic as, the observed differences for Na^+ ion. The observed differences are primarily due to the differences in the sizes and stability of the hydrated Na^+ and Cl^- ions.

5. Distribution of ions and water inside the tube: Effect of surface corrugation

We examine the effects of the architecture of the tube surface on the water molecules in the tube. Do the water molecules feel the atomic nature of the tube surface? We show this by projecting the water positions onto the internal wall surface of the nanotube and then use the periodicity of surface atoms to map the water positions onto the hexagon of the carbon nanotube structure. The results are shown in Fig. 6(a) for the tube containing three ion pairs (tube 6). Although all the water molecules, including the ones in the center column, are included in this analysis, the latter constitute only a small fraction of the total number of water molecules inside the tube. We find that the water molecules do feel the surface corrugation of the tube. The Na^+ and Cl^- ions also feel the surface corrugation, as seen in Figs. 6(b) and 6(c), although the latter has lower resolution than Fig. 6(a) because there are only three of each ion in the tube with 49 water molecules. Nevertheless, the Na^+ ions show preference for the center of the hexagon and just inside the six sides. The maximum in the radial profile of the Cl^- ion is between the center column of water and the cylindrical shell of water and thus spends most of its time farther away from the wall than Na^+ ion does. Indeed the Cl^- ion probability contours in Fig. 6(c) have less definition than that of Na^+ ion and do not appear to be influenced by the surface corrugation. Our results point to the importance of including the atomistic nature of the carbon nanotube (rather than a smooth tube) to capture the correct distribution of both water and ions in such systems.

6. Effects of the flexibility of the tube on distributions

Our carbon nanotubes are not only atomistic, they are *flexible*. We report changes in ion dynamics arising from the flexibility of the nanochannel. And we compare pure water results with results of Andreev *et al.*[59] who studied the effect of flexibility on behavior of water in (6,6)-type nanotubes by multiplying the C–C interaction potential terms by a damping factor $10^{-\phi}$. We changed the harmonic displacement force constant for tethering of the carbons of our nanotube by an order of magnitude to greatly enhance the flexibility. We find that the average occupancy number of the tube is less by about 6%. The first maxima in the $g(r_{NaO})$ and $g(r_{ClO})$ and the size of the first hydration shell are independent of the degree of flexibility of the tube, which is not surprising, since these quantities hardly change in going from the bulk

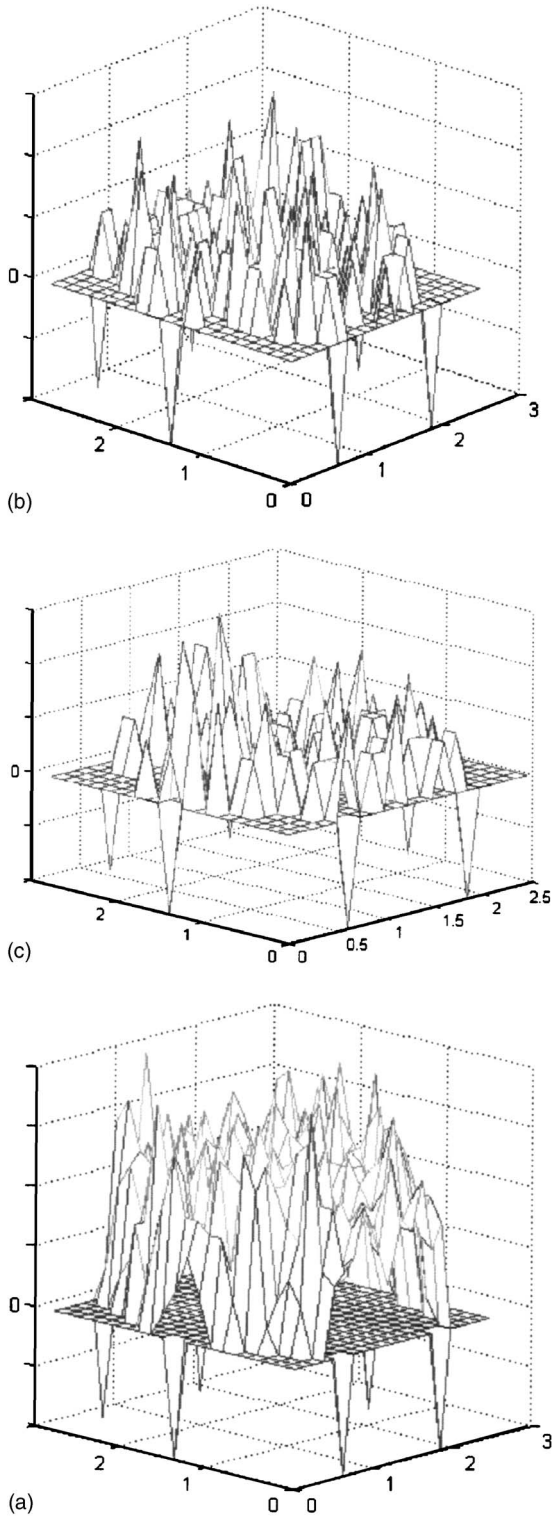

FIG. 6. Probability contours projected onto the graphene unit of the tube surface. (The six negative peaks mark the positions of the six carbons which constitute a hexagon.) (a) For H_2O, (b) for Na^+ ions, and (c) for Cl^- ions.

solution to inside the nanotube. The average hydration numbers for both ions are greater for the more flexible tube: 3.9 compared to 3.5 for Na^+ and 7 compared to 6.1 for Cl^-. Upon entering the more flexible tube, the ions do not lose as many waters from their first hydration shell as they do in the less flexible tube.

An interesting observation is that the radial density pro-

files of Na^+, Cl^-, and water, seen in Fig. 4 to be narrow and orderly when there are only one or two ions in the tube, become less so in the more flexible tube. In the more flexible tube, the Cl^- ions are also found close to the center line of the tube. With increasing number of ion pairs in the tube, the Cl^- ion density profile changes more than it does in Fig. 5(c). The Na^+ ion density profile in the more flexible tube changes with increasing number of ions in a similar manner as shown in Fig. 5(b).

B. Dynamics

1. Ion trajectories and permeation events

We examine in Figs. 7(a)–7(h) the trajectories of several ions which have entered a given tube by plotting their trajectories along the direction of the axis of the tube, including some number of time steps prior to entering the tube, and carrying the ions through to the end of the simulation, at which time most ions have not exited the tube. The trajectories of ions which are inside a tube at the same time are plotted together. We also examine whether the effective diameter (0.90 nm) of the tube is large enough to permit one hydrated ion to pass another in the tube. How is the nature of the ion dynamics inside the tube affected by the presence of other ions in the tube?

We find that two ions with the same charge tend to move along the tube direction in a correlated manner, whereas oppositely charged ions can pass each other in the tube. Note, for example, the Cl^- and Na^+ in Fig. 7(a). We never observed two Na^+ ions pass each other in any of the tubes, while there are instances in which two Cl^- ions passed each other in the tube [in Fig. 7(e) and also in Fig. 7(f)]. It is also observed that sets of oppositely charged ions tend to stay together in ion pairs, in Figs. 7(b), 7(e), and 7(g). Nicholson and Quirke have observed ion pairing in NaCl solutions in smooth cylindrical tubes, the nature and location being highly dependent on the tube diameter.[38] The ordering of ions along the direction of the channel remains very stable over a long period of time.

We observe that the rate of progress of an ion along the axial direction is affected by the presence of other ions. See, for example, Figs. 7(b), 7(e), and 7(f), in which the first ions to enter the tube moved farther along the axial direction when new ions entered the tube. We find that with only one ion pair (or only one ion) in the tube, no ionic permeation is observed; the ions tend to remain at a stable position along the axis of the tube (within ±0.2 nm). On the other hand, with two or three ion pairs present in the tube, one or two ions are observed exiting the tube. It appears from our simulations that in the absence of external electric fields, for a carbon nanotube possessing no surface charges, 2.36 nm in length and 0.90 nm in effective diameter, positive or negative ions will exit the tube only when one or two other ions of the same charge are present in the tube. We find that the permeation mechanism in these carbon nanotubes involves the presence of multiple ions in the tube, and Coulomb repulsion among the ions plays an essential role. Biological ion channels have been crystallized with two or two ions in the channels, and it has been proposed that at least three ion sites (close to the internal mouth, in the center, and close to the external mouth of the channel) in a Cl^- ion channel,[6] six in a K^+ ion channel,[60] can be deduced. The general mechanism of permeation which has been suggested for biological ion channels by previous workers at various levels of detail (see, for example, Refs. 8, 61, and 62) is that a like-charged ion entering the pore causes the ions preexisting in the pore to be displaced toward the exit in a concerted multi-ion process. This mechanism is observed here, without benefit of ion sites (ion-coordinating ligands) or surface charges. Thus, the mechanism of translocation assisted by Coulomb repulsion in a concerted multi-ion process appears to be a general one for ion transport through a membrane of hydrophobic channels, even in the absence of surface charges or specific ion sites.

We do not have a sufficient number of exiting events to permit a determination of translocation rate. Nor can we estimate the average time of transit from the entrance to the exit for a given ion from the simulations that we have carried out.

2. Effects of the flexibility of the tube on ion dynamics

The simulations for the more flexible tube (force constant multiplied by 0.1) were run using the same seed in the random number generator as in the standard runs shown above, so that the ions enter the tubes at the same point. In this way, we can compare directly the trajectories with those in Fig. 7. There were no large changes in the trajectories of ions in the tubes upon increasing the flexibility, except in those tubes with multiple ion pairs, i.e., tubes 5, 6, and 7. These trajectories are shown in Figs. 8(a)–8(c), which may be compared directly with Figs. 7(e)–7(g), respectively. The alternating sign ordering of the ions along the tube axis in those tubes with two or three ion pairs which was observed in Figs. 7(e) and 7(f) is preserved in the more flexible tube. There are considerably more incidences of ions passing each other along the tube axis in the more flexible tube. In contrast to the more rigid tube, there were far fewer incidences of ions exiting the more flexible tubes. It appears that flexibility of the tube tends to decrease the permeation rate.

3. Dynamics of water molecules in the first hydration shell

(a) *Exchange dynamics of water in the first hydration shell*. We define the exchange time as the average time for a water molecule in the first hydration shell of a particular ion to be exchanged. This is a measure of the stability of the solvated ion cluster. It is known from previous studies that the stability of Na^+-H_2O ion clusters is greater than that of Cl^--H_2O ion clusters in bulk solutions.[12] We find that this is also the case under confinement. Inside the tube, the average exchange time for the waters around Na^+ ion is longer (140.6 ps) than that of Cl^- ion (70.2 ps). The average exchange times of both types of ion clusters are longer inside the tube than in the bulk (8.2 ps for Na^+ ion, 4.0 ps for Cl^- ion). Very stable Na^+-H_2O ion clusters are formed inside the

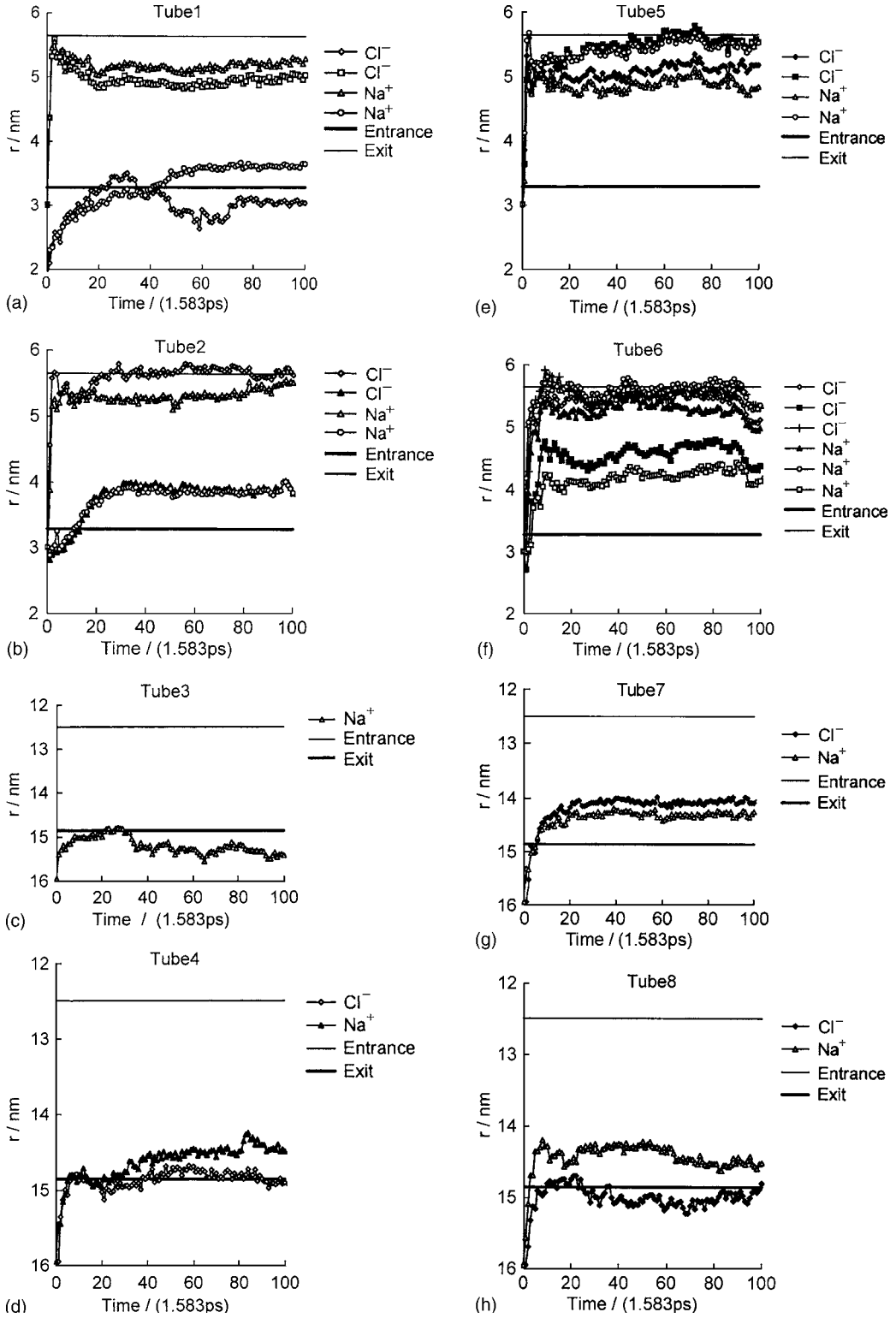

FIG. 7. Trajectories of ions in each of the eight tubes. (a) In tube 1 which ended with $2Na^+$, $1Cl^-$, and $54H_2O$. (b) In tube 2 which ended with $2Na^+$, $2Cl^-$, and $55H_2O$. (c) In tube 3 which ended with only 54 H_2O. (d) In tube 4 which ended with $1Na^+$, $0Cl^-$, and $56H_2O$. (e) In tube 5 which ended with $2Na^+$, $2Cl^-$, and $49H_2O$. (f) In tube 6 which ended with $3Na^+$, $3Cl^-$, and $49H_2O$. (g) In tube 7 which ended with $1Na^+$, $1Cl^-$, and $55H_2O$. (h) In tube 8 which ended with $1Na^+$, $1Cl^-$, and $53H_2O$.

nanotubes. And both types of ion clusters are more stable in nanotubes than in the bulk solution primarily because confinement restricts the number of water molecules available for exchange in these clusters.

(b) *Reorientation dynamics of water molecules in the first hydration shell*. The orientational correlation time of water molecules in ionic solutions has been measured with femtosecond pump-probe experiments which observe the waters in the first hydration shell of the anion and the water molecules outside this first shell separately.[63–66] The time constant that they obtain is τ_2, the decay time of the second order correlation function, $C_2(t)=\langle P_2(\mathbf{e}(t))\cdot P_2(\mathbf{e}(0))\rangle$. The

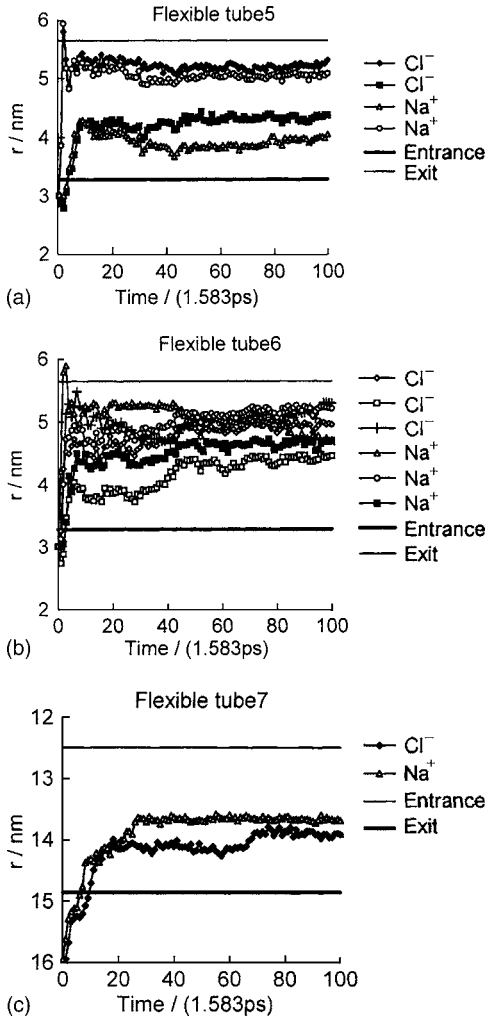

FIG. 8. Trajectories of ions in the more flexible tubes. (a) In tube 5 which ended with $2Na^+$, $2Cl^-$, and $53H_2O$. (b) In tube 6 which ended with $3Na^+$, $3Cl^-$, and $51H_2O$. (c) In tube 7 which ended with $1Na^+$, $1Cl^-$, and $52H_2O$.

reorientation time in this experimental study corresponds to τ_2 with **e** directed along the O–H bond. Experiments revealed that the first solvation shell of Cl^- ion has slower water reorientation dynamics (τ_2=9.6 ps at 298 K)[65] than the bulk water (τ_2=2.6 ps at 298 K),[63] while the dynamics of the water molecules outside the first hydration shell are observed to be negligibly affected by the ions. In previous classical MD studies, τ_2 time constants between 0.7 and 1.7 ps were found in bulk water,[67,68] whereas *ab initio* MD values were from 1.2 to 9 ps.[69]

In this work we calculated the reorientation time constant for the waters in the first hydration shell of Na^+ ions and Cl^- ions using an overlapped data procedure.[70] In bulk solution we find that the reorientation times for waters in the first hydration shell of both Na^+ and Cl^- ions (1.06 and 1.36 ps, respectively) are longer than for water molecules that are not associated with any ions (0.69 ps). Only the result for the anion may be compared with the femtosecond pump-probe experiments: Our results do agree with the experimental observation that reorientation times in the first hydration shell are longer than those for water molecules outside the first shell. Our important results are for water molecules confined in carbon nanotubes: We find that the time constant for the first hydration shell of Na^+ ion is longer in the tube (8.52 ps) than for the first hydration shell of Na^+ ion in the bulk solution (1.06 ps). It is also the case for the first hydration shell of Cl^- ions that the time constant is longer in the tube (8.65 ps) than in the bulk solution (1.36 ps). In confinement, the reorientation times of water molecules in the first hydration shell of both ions are slightly shorter than for water molecules that are not associated with any ions (8.87 ps). These results are summarized in Table II.

IV. DISCUSSION

Tubes which have smaller diameters such as to be able to support only a column of water along the axis of the tube cannot permit ions to enter because there is no space enough to accommodate the hydration shell; the desolvation of such ions imposes a large energy as well as entropic penalty. The 0.82 nm diameter tube has a large enough cross section to support both hydrated Na^+ and Cl^- ions since it can maintain both the central column of water and the cylindrical shell. In the 0.90 nm tubes, (Fig. 4) the Na^+ and Cl^- ions do not spend a significant fraction of time at the center line of the tube. Thus, previous simulations which fix a single positive ion in the center of the tube[44,45] are not likely to provide realistic results for these systems. In other single ion studies where the ion is free to move, the relative positions of the maxima in the ion and water profiles have been shown to depend on the diameter of the tube.[71] For model cylindrical tubes ranging in diameter from 0.42 to 1.12 nm, the outermost cylindrical water shell was found about 0.15 nm from the wall. Only in the smallest diameter tubes do the water and Na^+ ion profiles have considerable overlap. The Na^+ ion profile appears to change with tube diameter in such a way as to lie between the water profiles so as to maintain its first hydration shell.

Hansen and co-workers provide cation trajectories versus time for several permeation events. They found from the mean square displacements of solvated ions that diffusive motion occurs in the bulk but the ions have approximately constant velocity while within the pore. This may not happen in an equilibrium system. Hansen and co-workers,[34,35] studied permeation events only under nonequilibrium conditions. Their simulation of ion transport is under conditions of *ion imbalance*, with one reservoir net negatively and the other net positively charged, i.e., with different number of cations and anions in the two reservoirs, they have an imposed electric field which continuously changes as each ion exits the tube.

Our ion trajectories are obtained under the conditions in which two compartments are electrically neutral at the beginning of the simulation, and our carbon nanotubes have no surface charges. Furthermore, our ion trajectories permit comparison under the same conditions since the trajectories in all eight tubes are observed under exactly the same reservoir conditions. In this way the trajectories in a tube containing three ion pairs can be directly compared with those in a tube containing two ion pairs or one ion pair. Our results are more general than those of Peter and Hummer in that our ions are not constrained to stay inside the tube, or fixed at the

TABLE II. Water reorientation and exchange times.

	In tube			In bulk		
Time (ps)	In Na^+ first hydration shell	In Cl^- first hydration shell	Water not associated with ions	In Na^+ first hydration shell	In Cl^- first hydration shell	Water not associated with ions
Exchange time, this work	140.6	70.2	···	8.2	4.0	···
Reorientation time, this work	8.52	8.56	8.87	1.06	1.36	0.69
Reorientation time, expt.					9.6[a]	2.6[b]
Reorientation time, other MD				19.9–25.5[c]	11.4–15.5[c]	0.7–1.7[d] 1.2–9[e]

[a]Reference 65.
[b]Reference 63.
[c]Reference 85.
[d]References 67 and 68.
[e]Reference 69.

center of the tube, or tethered in the axial direction. Thus, our ion radial density profiles, hydration shell structures, and trajectories are for ions in transit and not artificially constrained.

As seen in Fig. 5(c), as the number of ions in the tube increases, the Cl^- ion radial profile does tend to spread slightly, whereas the Na^+ radial profile dramatically spreads towards the center line. This is how ions of opposite charge can pass each other; the Na^+ ion can move towards the center of the tube to accommodate having a Cl^- ion in the same cross-sectional plane. Examination of a sequence of snapshots in Fig. 9 provides the mechanism which facilitates this passing. We see that in the confined space of the 0.90 nm nanotube, the Na^+ and Cl^- ions pass each other by sharing an expanded hydration shell which re-forms around each ion as they move away from each other. In a biological channel, the coordination number of a K^+ ion or a Na^+ ion would remain fairly constant (6-8 and 5-6, respectively) as it sheds water molecules when it moves into the coordination influence of protein carbonyl or hydroxyl groups.[72] In a similar fashion, in our simulations, in the tubes containing Na^+ and Cl^- ions, the Na^+ ion is able to maintain its coordination number while passing a Cl^- ion by the reorganization of the water molecules around both ions, so that for a short time, the Cl^- substitutes for a water molecule in Na^+ ion's first hydration shell. Figure 9 shows three snapshots of one ion pair in tube 5. The water molecules are shown in red, Na^+ ions are blue, and Cl^- ions are green. At the end of this simulation, the ions still form one ion pair.

We have presented results for both water reorientation times and water exchange times under confinement in comparison to the bulk. The reorientation time constant and the exchange times of waters in the first hydration shell are related to each other because hydrogen bonds have to be broken and re-formed in both reorientation and exchange. However, since we have not included polarization in our model for water, we cannot examine this relationship because we do not have accurate representation of hydrogen-bond breaking and re-forming events.

Several experimental investigations have contributed to understanding of water in confinement in nanoscopic volumes.[73–76] transmission electronic microscopy (TEM) observations of water confined in multiwall nanotubes[73] do not provide sufficient detail to be useful as tests of simulations, however. Atomic force microscopy has been used to form and manipulate a nanometric column of water molecules and make measurements of its elasticity.[74] Neutron scattering of water inside single-walled nanotubes has provided insight into the structure of nanotube water. [77] There have been studies of water confined in reverse micelles which are nanoscopic cavities created by surfactant molecules oriented such that their polar head groups point inward toward the aqueous phase. Frequency-resolved pump-probe infrared experiments have been carried out on HOD water in reverse micelles in which the nanopool sizes are 4.0, 2.6, and 1.7 nm in diameter, containing approximately 1000, 300, and 50 water molecules.[75] These experiments examined the influence of confinement on the orientational dynamics of water as a function of the size, and these results were compared to the identical experiments in bulk water, revealing that the dynamics of water in confinement was not at all bulklike. We have found that the dynamics of water in tubes 0.90 nm in diameter is different from dynamics of water in bulk water by various measures such as reorientation times.

In experiments using femtosecond pump-probe spectroscopy for the determination of the orientational relaxation of water molecules as a function of distance from an anion in bulk solutions, it has been shown that the effect of an anion on water structure is highly localized,[64] Omta *et al.* selectively probed water molecules that reside either in the primary hydration shell or in the more distant bulk water. All water molecules detected outside this shell were found to

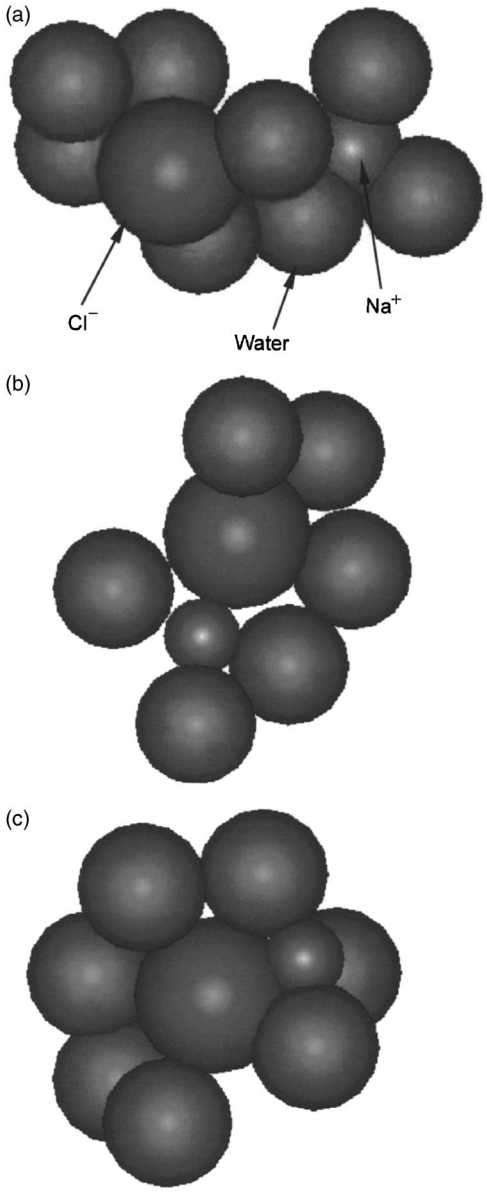

FIG. 9. Snapshots of solvation shells of Na^+ and Cl^- ions as they pass each other in the carbon nanotube.

have relaxation rates that are identical to that of the pure liquid water and independent of the concentration of the solute. In other words, they observe a very local effect of the ion on the dynamics of water molecules in bulk solution. Our simulation results are in agreement with the experimental result that the reorientation times of water molecules in the first hydration shell of an ion are longer than the reorientation time of water molecules not associated with ion clusters.

Some features of the structure of solvated ions in bulk are known from experiments.[78] Hydration numbers determined by diffraction methods in bulk and those obtained in molecular dynamics simulations are not always the same even though the structure found in both methods are very similar. In the diffraction methods, the hydration number is evaluated from the area under the relevant Gaussian-type peak, whereas in simulations, the first hydration shell is conventionally defined as the region from $r=0$ up to the first minimum in $g(r)$ after passing the first maximum. The hydration number of Na^+ measured by the diffraction methods is distributed over the range of 4–8. Computer simulations, on the other hand, range from 4.6 to 6.0.[49–54] We obtained a hydration number of 4.5. The Na–O length determined by diffraction methods falls in a relatively narrow range of 0.240–0.250 nm, whereas computer simulations find 0.235–0.245 nm.[49,50,52,54] Our value is 0.228 nm. Many x-ray and neutron diffraction measurements show that Cl^- ion is hydrated with six water molecules. Various previous simulations in bulk solutions report hydration numbers of 5.6–7.5.[49,51,55] Our value is 6.3. Computer simulations suggest that the hydration structure around Cl^- is not so definite since the peak found in the $g(r)$ function is very asymmetric and the running coordination number has no plateau. The Cl–O length is determined to be 3.10–3.20 Å from diffraction measurements. The position of the first maximum in $g(r)$ in computer simulations ranges from 0.320 to 0.322 nm for Cl^- ion.[48,49] Our value is 0.304 nm.

The residence time of water molecules in the first hydration shell of ions has not been determined experimentally, although reorientation correlation times associated with orientational relaxation have been studied via femtosecond studies such as those by Omta *et al.*[66] Our MD simulations provide a measure of substitution rates of water in the first hydration shell in the form of exchange times, i.e., the average time for one of the water molecules in the first hydration shell to change identity. It has been suggested that the breakup of the first hydration shell is initiated by molecular reorientation rather than by translation. [79] If this is accurate, then the time for exchange of waters in the first hydration shell should correlate with reorientation times of waters in the first hydration shell. We find this average exchange time to be 8.2 ps for Na^+ ion and 4.0 ps for Cl^- ion in the bulk solution. Results of MD simulations relevant to this exchange time are often reported in terms of the residence time, calculated from integration of time correlation functions of 1 or 0 if in the first hydration shell or not.[49,79] Various values of residence times have been reported for water in the first hydration shell of Na^+: 18.5–27.0 ps, increasing with ion concentration,[80] 23.8 ps for a rigid water model and 38.5 for flexible water,[81] the flexibility of the water decreases the speed of reorientation, 26.4 or 35 ps, depending on the water model,[49] 19.6 or 22.4 ps, depending on whether a lag time is included,[82] and 30 ps at room temperature and changing with temperature.[48] For water in the first hydration shell of Cl^-: 9.0 ps,[49] 10.0–14.3 ps, increasing with concentration,[80] and 12.8 or 16.6 ps, depending on whether a lag time is included.[82] MD simulations thus reveal that residence times of water in the first hydration shell of Cl^- are shorter by about a factor of 2 compared to that in the hydration shell of Na^+ ion. In agreement with these other simulations, our relative values for water exchange times in the first hydration shells of Na^+ and Cl^- ions in bulk solution are in a ratio of 2.05.

Experiments on confined ionic solutions are rarer. Neutron spin echo measurements probe the dynamics of a quasi-two-dimensional water with layer thickness corresponding to two molecular layers with Na^+ ions trapped in crystalline Na vermiculite platelets at separations of precisely 1.49 nm.[76]

The authors find that there are about seven water molecules per interlayer Na^+ ion, and they find the water dynamics considerably slower than has been observed in the bulk at the same temperature. Our results in Table II are in agreement with this: Exchange times and reorientation times are longer in confinement than in the bulk solution. They also find a broad distribution of relaxations, for waters in different local environments, interacting with the clay, with the Na^+, and with other water. In another study, surface force balance experiments were carried out on NaCl solution trapped between two flat mica surfaces compressed down to a gap of 1 nm.[83] Here the gap between the surfaces is occupied mostly by water molecules bound to surface-attached ions and some free hydrated ions of the solution. The resulting shear forces are characteristic of a fluidity that is not too far removed from that of bulk water. They attribute this observation to the exchange of water molecules at the outer surfaces of the two bound hydration layers. To the best of our knowledge, these two are the only experiments on confined solvated ions. Our simulation results provide detailed information for the hydrated anions in confinement that could be tested by experiments, for example, the same femtosecond experiments done in bulk solution by Omta *et al.* could be carried out for ions confined in nanotubes, provided the infrared peaks are sufficiently resolved.

Inside a biological channel, the coordination numbers are maintained by coordination with protein. The number of water molecules in the first coordination shell fluctuates, with the number of waters being smallest when the ion is at the binding region which serves as the selectivity filter. For example, in molecular dynamics simulations of the anion-selective Omp32 channel, the coordination number of the Cl^- ion fluctuates along the channel, with contributions coming from both water and protein.[84] The average is 6.2, ranging from 5.5 to 6.5, except at the binding region, where the coordination number gets up to a maximum of 8, of which 3.0–5.5 come from water coordination. The same has been found in simulations in K^+ ion channels, where the coordination number of K^+ ion is 6–8 whereas that of Na^+ ion is 5–6.[72] The ability of biological ion channels to discriminate between different ions such as K^+ versus Na^+ is conventionally attributed to the geometry/size constraints of selectivity filters which are integral parts of the channel structure. In simulations in model systems such as the present study, where no special selectivity filters are included in the model, it is possible to find out more general concepts, such as how structure of coordination shells, exchange/reorientation of coordinated solvent molecules, and ion dynamics are influenced by confinement in channels having dimensions similar to biological channels.

V. CONCLUSIONS

The water molecules of the first hydration shell of both ions exchange less frequently inside the tube than in the bulk solution. The water molecules of the hydrated Na^+ ion exchange less frequently than the waters of the hydrated Cl^- ion whether inside the nanotubes or in the bulk solution. This is obviously governed by the fewer available water molecules in confinement, compared to in bulk. Our results for the hydration shell structure in confinement are general and have been averaged over all the tubes with various numbers of ions present. The first hydration boundaries of Na^+-H_2O or Cl^--H_2O ion clusters are the same inside the nanotubes as found in the bulk, and this did not change in our study inside nanotubes of different diameters. The first shell of Na^+-H_2O ion clusters in the carbon nanotubes has fewer water molecules than that in the bulk although their first shell boundary is almost the same. There is no big difference for Cl^--H_2O ion clusters inside the nanotubes compared with that in the bulk solution. That the first hydration shell of Na^+ ion can have as much as one or more H_2O molecule fewer compared to that in bulk solution is interesting. Clearly, ion passage through biological channels requires water molecules, especially in the hydrophobic regions.The effects of the flexibility of the tube become most evident when the tube is inhabited by multiple ions. The average hydration numbers for both ions are greater for the more flexible tube: 3.9 compared to 3.5 for Na^+ and 7 compared to 6.1 for Cl^-. Upon entering the more flexible tube, the ions do not lose as many waters from their first hydration shell as they do in the less flexible tube.

Our most significant results are the comparisons of trajectories and radial distribution profiles for various numbers of ions in the tube, all of which were observed simultaneously under the same reservoir conditions, since we have eight tubes constituting the membrane in our simulation box. We find that although hydrated ions of the same charge move in single file in the tube, ions of opposite charge can pass each other in the tube. The trajectories show this explicitly, and the radial profiles clearly show that when there are multiple ions in the tube, the Na^+ ion radial density profile spreads out toward the center of the tube, while the Cl^- ion radial profile does not spread very much. The Na^+ ion can move towards the center of the tube to accommodate having a Cl^- ion in the same cross-sectional plane. In the confined space of the 0.90 nm nanotube, the Na^+ and Cl^- ions pass each other by sharing an expanded hydration shell which re-forms around each ion as they move away from each other. There are considerably more incidences of ions passing each other along the tube axis in the more flexible tube.

We find that events of ions exiting the channel can occur only when multiple ions are present in a tube. Thus, the permeation mechanism involves multiple ions, and Coulomb repulsion among the ions plays an essential role in a general case of a hydrophobic tube without external electric field or surface charges. Multiple ion involvement in transport had been suggested for biological ion channels. Since our tubes have no surface charges or ligand groups which could serve as binding sites, then we can say that this permeation mechanism has only to do with the nature of hydrated ions under confinement in hydrophobic cylindrical tubes and is not specific to biological channels. We are now carrying out MD simulations of hydrated ions in surface-charged carbon nanotubes which we can compare directly with the present results in order to investigate how ion transport is affected by surface charges in neutral tubes and by surface charges in tubes with a net charge. The latter are relevant to ion transport in

one-dimensional channeled zeolite membranes where the zeolite framework itself has a net charge determined by the extent of Al substitution for Si and also in the design of nanofluidic systems that use electro-osmotic transport as a primary means of fluidic transport.[15–17] Characteristics of flow in carbon nanotubes can be vital for generating the high throughput rates required in nanofluidic devices employing carbon nanotubes.[18]

ACKNOWLEDGMENTS

This research has been funded by the National Science Foundation [Grant Nos. CHE-9978259 (for C.J.J.) and CTS-0314203 (for S.M.)], DOE [Grant No. DE-FG02-96ER14680 (for S.M.)], and the Petroleum Research Fund of the American Chemical Society (for S.M.). The authors thank Professor Sarah Gerber (Rosalind Franklin University) for helpful discussions on anion channels.

[1] R. McKinnon, Angew. Chem., Int. Ed. **43**, 4265 (2004).
[2] P. Agre, Angew. Chem., Int. Ed. **43**, 4278 (2004).
[3] P. C. Jordan, IEEE Trans. Nanobiosci. **4**, 3 (2005).
[4] G. V. Miloshevsky and P. C. Jordan, Trends Neurosci. **27**, 308 (2004).
[5] R. Dutzler, E. B. Campbell, M. Cadene, B. T. Chait, and R. MacKinnon, Nature (London) **415**, 287 (2002).
[6] R. Dutzler, E. B. Campbell, and R. MacKinnon, Science **300**, 108 (2003).
[7] B. Corry, M. O'Mara, and A. H. Chung, Biophys. J. **86**, 846 (2004).
[8] J. Cohen and K. Schulten, Biophys. J. **86**, 836 (2004).
[9] G. V. Miloshevsky and P. C. Jordan, Biophys. J. **86**, 825 (2004).
[10] A. Suenaga, J. Z. Yeh, M. Taiji *et al.*, Biophys. Chem. **120**, 36 (2006).
[11] K. Liu, D. Kozono, Y. Kato, P. Agre, A. Hazama, and M. Yasui, Proc. Natl. Acad. Sci. U.S.A. **102**, 2192 (2005).
[12] S. Murad and J. Lin, Ind. Eng. Chem. Res. **41**, 1076 (2002).
[13] S. Murad, W. Jia, and M. Krishnamurthy, Mol. Phys. **102**, 2103 (2004).
[14] *Technical Proceedings of the 2005 NSTI Nanotechnology Conference, Nanotech, Anaheim, CA, 8–12 May 2005* (PSTI, Danville, CA, 2005), Vol. 1, Chap. 10, p. 1.
[15] T. Kuo, L. Sloan, J. Sweedler, and P. Bohn, Langmuir **17**, 6298 (2001).
[16] P. Kemery, J. Steehler, and P. Bohn, Langmuir **14**, 2884 (1998).
[17] M. Majumder, N. Chopra, and B. J. Hinds, J. Am. Chem. Soc. **127**, 9062 (2005).
[18] S. Niyoge and R. C. Haddon, Proc. Natl. Acad. Sci. U.S.A. **101**, 6331 (2004).
[19] G. Hummer, J. C. Rasaiah, and J. P. Nowortya, Nature (London) **414**, 188 (2001).
[20] D. Lu, Y. Li, S. V. Rotkin, U. Ravaioli, and K. Schulten, Nano Lett. **4**, 2383 (2004).
[21] R. J. Mashl, S. Joseph, N. R. Aluru, and E. Jakobsson, Nano Lett. **3**, 589 (2003).
[22] A. Waghe, J. Rasaiah, and G. Hummer, J. Chem. Phys. **117**, 10789 (2002).
[23] D. J. Mann and M. D. Halls, Phys. Rev. Lett. **90**, 195503 (2003).
[24] C. Dellago, M. Naor, and G. Hummer, Phys. Rev. Lett. **90**, 105902 (2003).
[25] J. Wang, Y. Zhu, J. Zhou, and X.-H. Lu, Phys. Chem. Chem. Phys. **6**, 829 (2004).
[26] A. Striolo, K. E. Gubbins, A. A. Chialvo, and P. T. Cummings, Mol. Phys. **102**, 243 (2004).
[27] J. Marti and M. C. Gordillo, Chem. Phys. Lett. **354**, 227 (2002).
[28] J. Marti, E. Guardia, and M. C. Gordillo, Chem. Phys. Lett. **365**, 536 (2002).
[29] M. C. Gordillo and J. Marti, Chem. Phys. Lett. **341**, 250 (2001).
[30] A. Kalra, S. Garde, and G. Hummer, Proc. Natl. Acad. Sci. U.S.A. **100**, 10175 (2003).
[31] S. Vaitheeswaran, J. C. Rasaiah, and G. Hummer, J. Chem. Phys. **121**, 7955 (2004).
[32] B. Huang, Y. Xia, M. Zhao, F. Li, X. Liu, Y. Ji, and C. Song, J. Chem. Phys. **122**, 084708 (2005).
[33] F. Q. Zhu and K. Schulten, Biophys. J. **85**, 236 (2003).
[34] J. Dzubiella, R. J. Allen, and J.-P. Hansen, J. Chem. Phys. **120**, 5001 (2004).
[35] J. Dzubiella and J.-P. Hansen, J. Chem. Phys. **122**, 234706 (2005).
[36] Y. W. Tang, K. Y. Chan, and I. Szalai, J. Phys. Chem. B **108**, 18204 (2004).
[37] R. M. Lynden-Bell and J. C. Rasaiah, J. Chem. Phys. **105**, 9266 (1996).
[38] D. Nicholson and N. Quirke, Mol. Simul. **29**, 287 (2003).
[39] C. Peter and G. Hummer, Biophys. J. **89**, 2222 (2005).
[40] S. Murad and J. G. Powles, J. Chem. Phys. **99**, 7271 (1993).
[41] B. Guillot, J. Mol. Liq. **101**, 219 (2002).
[42] M. P. Allen and D. J. Tildesley, *Computer Simulation of Liquids* (Clarendon, Oxford, 1987).
[43] D. J. Evans and S. Murad, Mol. Phys. **34**, 327 (1977).
[44] R. Allen, S. Melchionna, and J. P. Hansen, Phys. Rev. Lett. **89**, 175502 (2002).
[45] R. Allen, J. P. Hanson, and S. Melchionna, J. Chem. Phys. **119**, 3905 (2003).
[46] O. Beckstein and M. S. P. Sansom, Proc. Natl. Acad. Sci. U.S.A. **100**, 7063 (2003).
[47] I. Brovchenko and A. Geiger, J. Mol. Liq. **97**, 195 (2002).
[48] T. Driesner, T. M. Seward, and I. G. Tironi, Geochim. Cosmochim. Acta **62**, 3095 (1998).
[49] S. H. Lee and J. C. Rasaiah, J. Phys. Chem. **100**, 1420 (1996).
[50] S. Obst and H. Bradaczek, J. Phys. Chem. **100**, 15677 (1996).
[51] J. P. Noworyta, S. Koneshan, and J. C. Rasaiah, J. Am. Chem. Soc. **122**, 11194 (2000).
[52] M. Cascella, L. Guidoni, A. Maritan, U. Rothlisberger, and P. Carloni, J. Phys. Chem. B **106**, 13027 (2002).
[53] M. Carillo-Tripp, H. Saint-Martin, and I. Ortega-Blake, J. Chem. Phys. **118**, 7062 (2003).
[54] S. B. Rempe and L. R. Pratt, e-print physics/0006026.
[55] A. Tongraar and B. M. Rode, Phys. Chem. Chem. Phys. **5**, 357 (2003).
[56] M. Tanaka and M. Aida, J. Solution Chem. **33**, 887 (2004).
[57] M. C. Gordillo and J. Marti, Chem. Phys. Lett. **341**, 250 (2001).
[58] M. C. Gordillo and J. Marti, Chem. Phys. Lett. **329**, 341 (2000).
[59] A. Andreev, D. Reichman, and G. Hummer, J. Chem. Phys. **123**, 194502 (2005).
[60] Y. Zhou, J. H. Morais-Cabral, A. Kaufman, and R. MacKinnon, Nature (London) **414**, 43 (2001).
[61] A. L. Hodgkin and R. D. Keynes, J. Phys. A **128**, 61 (1955).
[62] S. Berneche and B. Roux, Nature (London) **414**, 73 (2001).
[63] H. K. Nienhuys, R. A. van Santen, and H. J. Bakker, J. Chem. Phys. **112**, 8487 (2000).
[64] A. W. Omta, M. F. Kropman, S. Woutersen, and H. J. Bakker, Science **301**, 347 (2003).
[65] H. J. Bakker, M. F. Kropman, and A. W. Omta, J. Phys.: Condens. Matter **17**, S3215 (2005).
[66] A. W. Omta, M. F. Kropman, S. Woutersen, and H. J. Bakker, J. Chem. Phys. **119**, 12457 (2003).
[67] A. Chandra and T. Ichiye, J. Chem. Phys. **111**, 2901 (1999).
[68] D. van der Spoel, P. J. van Maaren, and H. J. Berendsen, J. Chem. Phys. **108**, 10220 (1998).
[69] M. Sprik, J. Hutter, and M. Parinello, J. Chem. Phys. **105**, 1142 (1996).
[70] D. C. Rapaport, *The Art of Molecular Dynamics Simulation* (Cambridge University Press, Cambridge, 1995); D. Frenkel and B. Smit, *Understanding Molecular Simulation: From Algorithms to Applications* (Academic, San Diego, 1996).
[71] T. W. Allen, S. Kuyucak, and S. H. Chung, J. Chem. Phys. **111**, 7985 (1999).
[72] T. W. Allen, A. Bliznyuk, A. P. Rendell, S. Kuyucak, and S. H. Chung, J. Chem. Phys. **112**, 8191 (2000).
[73] N. Naguib, H. Ye, Y. Gogotsi, A. G. Yazicioglu, C. M. Megaridis, and M. Yoshimura, Nano Lett. **4**, 2237 (2004).
[74] H. Choe, M.-H. Hong, Y. Seo, K. Lee, G. Kim, Y. Cho, J. Ihm, and W. Jhe, Phys. Rev. Lett. **95**, 187801 (2005).
[75] H. S. Tan, I. R. Piletic, and M. D. Fayer, J. Chem. Phys. **122**, 174501 (2005).
[76] J. Swenson, R. Bergman, and S. Longeville, J. Chem. Phys. **115**, 11299 (2001).
[77] A. I. Kolesnikov, J. M. Zanotti, C. K. Loong, P. Thiyagarajan, A. P. Moravsky, R. O. Loutfy, and C. J. Burnham, Phys. Rev. Lett. **93**, 035503 (2004).

[78] H. Ohtaki and T. Radnai, Chem. Rev. (Washington, D.C.) **93**, 1157 (1993).
[79] R. W. Impey, P. A. Madden, and I. R. McDonald, J. Phys. Chem. **87**, 5071 (1983).
[80] S. Chowdhuri and A. Chandra, J. Chem. Phys. **115**, 3732 (2001).
[81] E. Guardia and J. A. Padro, J. Phys. Chem. **94**, 6049 (1990).
[82] S. Koneshan, S. H. Lee, R. M. Lynden-Bell, and J. C. Rasaiah, J. Phys. Chem. B **102**, 4193 (1998).
[83] U. Raviv and J. Klein, Science **297**, 1540 (2002).
[84] U. Zachariae, V. Helms, and H. Engelhardt, Biophys. J. **85**, 954 (2003).
[85] R. Chitra and P. E. Smith, J. Phys. Chem. B **104**, 5854 (2000).